

## A CUBIC B-SPLINE COLLOCATION METHOD FOR THE EW EQUATION

İdris Dağ<sup>\*</sup> and Bülent Saka<sup>\*\*</sup>

Osmangazi University,

Computer Engineering Department<sup>\*</sup>, Mathematics Department<sup>\*\*</sup>,  
26480, Eskişehir, Turkey. idag@ogu.edu.tr, bsaka@ogu.edu.tr

**Abstract-** A numerical solution of the Equal Width (EW) equation based on a collocation method incorporated cubic B-splines is investigated. Accuracy of the proposed method is shown numerically by calculating conservation laws,  $L_2$  and  $L_\infty$  norms on studying migration of a single solitary wave. It is shown that the collocation scheme for solutions of the EW equation gives rise to smaller errors and is quite easy to implement. The development of the undular bore and generation of the waves are studied for the EW equation. The linearized stability of the proposed method is derived by using Von Neumann stability analysis.

**Keywords-** Finite Elements, Collocation, Solitary Waves, EW Equation.

### 1. INTRODUCTION

Nonlinear dispersive wave equations exhibit fascinating solutions such as solitary waves and solitons. Existence of such solutions has been source of intense interest. Solution of those equations is not analytically available in general. So numerical solutions of those equations are needed in order to develop an understanding of the nonlinear phenomena. There are many different examples of these type equations, each modelling several different physical problems. We shall concentrate on the equal width (EW) equation whose solutions exhibits soliton like solutions. Main properties of those solutions are that solitary waves propagate in one direction with constant speed without changing its shape and that the solitary waves pass through one another and emerge unaltered in shape.

The present study is concerned with the numerical solution of the EW equation that has been suggested by Morrison et al. [4] and has the following form:

$$U_t + UU_x - \mu U_{xxt} = 0. \quad (1)$$

We take the EW equation (1) together with the artificial boundary conditions  $U(a,t)=\alpha_1$ ,  $U(b,t)=\alpha_2$  and  $U_x(a,t)=U_x(b,t)=0$  over the region  $a \leq x \leq b$  and initial condition  $U(x,0)$ .

The use of various degree of the B-splines in getting the numerical solution of the some partial differential equations are shown to provides easy and simple algorithms [5,6,7,8,9]. Various forms of finite element method incorporated with the B-splines as shape functions have been presented to give smooth solutions and these functions guarantees continuity of approximating functions at the mesh points up to one less degree of B-splines. Cubic B-spline Galerkin finite element method is applied to EW equation to model propagation and interaction of solitary waves [5,6]. By using the Petrov-Galerkin method using quadratic B-spline spatial finite elements, motion of solitary waves and development of the undular bore was studied [9]. The development of the solitary waves from an arbitrary initial condition for the EW equation is examined by using least squares technique using linear-space finite elements [5]. The development of a train of EW solitary waves induced by boundary forcing is revealed

by implementation of Petrov-Galerkin finite element method with shape functions taken as quadratic B-splines [11].

In the work, using cubic B-splines and method of collocation to solve the EW equation in section 2 develops an algorithm. Stability of the method is discussed in section 3. In the final section, a single solitary solution is studied to illustrate the accuracy and efficient of the proposed algorithm by calculating invariants,  $L_2$  and  $L_\infty$  norms. The undulation bore is visualized at long run of the algorithm. Results are compared with very recent papers [9, 10]. The effect of forcing boundary condition on the generation of solitary waves for the EW equation is illustrated.

## 2. THE B-SPLINE COLLOCATION METHOD

Let  $[a, b]$  be partitioned into a mesh by points  $x_1, x_2, \dots, x_N$  such that

$$a = x_0 < x_1 < \dots < x_{N-1} < x_N = b, \quad \text{where } h = x_{i+1} - x_i, \quad i=0, \dots, N-1. \quad (2)$$

The cubic B-splines will be used to approximate the solution  $U(x, t)$  of the equation (1). The cubic B-splines  $\phi_j$ ,  $j=-1, \dots, N+1$  at the nodes  $x_i$  are defined to form a basis over the interval  $[a, b]$  [2]. Thus, an approximation  $U_N$  to the exact solution  $U$  can be expressed in terms of the cubic B-splines as

$$U_N(x, t) = \sum_{j=-1}^{N+1} \delta_j(t) \phi_j(x), \quad (3)$$

where  $\delta_j$  are time dependent parameters to be determined from boundary conditions and collocation form of the differential equation. A cubic B-spline covers four elements (interval in the mesh).

$$\phi_j(x) = \frac{1}{h^3} \begin{cases} (x - x_{j-2})^3 & [x_{j-2}, x_{j-1}] \\ h^3 + 3h^2(x - x_{j-1}) + 3h(x - x_{j-1})^2 - 3(x - x_{j-1})^3 & [x_{j-1}, x_j] \\ h^3 + 3h^2(x_{j+1} - x) + 3h(x_{j+1} - x)^2 - 3(x_{j+1} - x)^3 & [x_j, x_{j+1}] \\ (x_{j+2} - x)^3 & [x_{j+1}, x_{j+2}] \\ 0 & \text{otherwise} \end{cases} \quad (4)$$

So the four cubic B-splines  $\phi_{j-1}, \phi_j, \phi_{j+1}, \phi_{j+2}$  lie in each element. Over the typical element  $[x_j, x_{j+1}]$ , the approximate  $U_N$  is given by

$$U_N = \sum_{i=j-1}^{j+2} \delta_i(t) \phi_i(x) \quad (5)$$

where  $\phi_i(x)$  act as element shape functions of the element, with the  $\delta_i(t)$  as element parameters. The form (5) shows the variation of all contributing cubic B-splines over a single element and is useful for working out the solution inside the element.

The nodal values of  $U$  and derivatives  $U', U''$  at the nodes are determined in term of the element parameters  $\delta_j$  by

$$U(x_j) = \delta_{j-1} + 4\delta_j + \delta_{j+1}, \quad hU'(x_j) = 3(\delta_{j+1} - \delta_{j-1}), \quad h^2U''(x_j) = 6(\delta_{j-1} - 2\delta_j + \delta_{j+1}) \quad (6)$$

where the symbol ' denotes the differentiation with respect to  $x$ .

Assume that the vector  $\mathbf{d} = (\delta_{-1}, \delta_0, \dots, \delta_N, \delta_{N+1})$  identifies the all element parameters. With a Crank-Nicholson approach in time,  $\mathbf{d}$  is linearly interpolated

between two time levels  $n$  and  $n+1$  and time derivative  $\frac{d\mathbf{d}}{dt}$  is discretised using the standard finite difference scheme so that

$$\mathbf{d} = \frac{1}{2}(\mathbf{d}^n + \mathbf{d}^{n+1}), \quad \frac{d\mathbf{d}}{dt} = \frac{1}{\Delta t}(\mathbf{d}^{n+1} - \mathbf{d}^n), \quad (7)$$

where  $\mathbf{d}^n$  are the parameters at the time  $n\Delta t$  and  $\Delta t$  is the time step.

The collocation points are selected to be coincident with the nodes (2). Substituting expression (3) into eq. (1), and using the eqs. (6) and (7) lead to a system equation:

$$\alpha_{j1}\delta_{j-1}^{n+1} + \alpha_{j2}\delta_j^{n+1} + \alpha_{j3}\delta_{j+1}^{n+1} = \alpha_{j3}\delta_{j-1}^n + \alpha_{j2}\delta_j^n + \alpha_{j1}\delta_{j+1}^n, \quad j = 0, 1, \dots, N \quad (8)$$

where  $\alpha_{j1} = 1 - R_1 - R_2 z_j$ ,  $\alpha_{j2} = 4 + 2R_1$ ,  $\alpha_{j3} = 1 - R_1 + R_2 z_j$ ,

$$R_1 = \mu \frac{6}{h^2}, \quad R_2 = \frac{3\Delta t}{2h}, \quad z_j = \delta_{j-1} + 4\delta_j + \delta_{j+1}.$$

The system above consists of  $N+1$  equations including  $N+3$  unknowns  $\mathbf{d}^n = (\delta_{-1}^n, \delta_0^n, \dots, \delta_N^n, \delta_{N+1}^n)$ .

We need to add two accepted boundary conditions  $U(a, t) = U(b, t) = 0$  to obtain a unique solution of this system. Using those boundary conditions, the parameters  $\delta_{-1}^n, \delta_{N+1}^n$  are eliminated from this system. Following recurrence relationship for time parameter vectors  $\mathbf{d}^n$  from the system (8) can be written in matrix form with

$$A(\mathbf{d})\mathbf{d}^{n+1} = B(\mathbf{d})\mathbf{d}^n + \mathbf{r}, \quad (9)$$

where  $A(\mathbf{d})$  and  $B(\mathbf{d})$  are  $(N+1) \times (N+1)$  tridiagonal matrices and  $\mathbf{r}$  is a vector obtained from the boundary conditions.

Since matrices  $A$  and  $B$  depend on  $\frac{1}{2}(\mathbf{d}^{n+1} + \mathbf{d}^n)$ , the iteration steps below are adopted to cope with the non-linear term induced by matrices  $A(\mathbf{d})$  and  $B(\mathbf{d})$ ,

\* Approximate  $A$  and  $B$  by  $A^*$  and  $B^*$  derived from  $\mathbf{d}^* = \mathbf{d}^n + \frac{1}{2}(\mathbf{d}^{n+1} - \mathbf{d}^n)$

\* Iterate two or more times to redefine the approximation to  $\mathbf{d}^{n+1}$ .

To evaluate the time development of  $\mathbf{d}^n$  in the system (9), initial condition  $\mathbf{d}^0$  needs to be determined from the initial condition  $U(x, 0)$  which can be approximated by the cubic B-splines over  $[a, b]$

$$U_N(x, 0) = \sum_{j=-1}^{N+1} \delta_j^0(t) \phi_j(x), \quad \text{where } \delta_j^0 \text{ are unknown parameters.}$$

To determine the parameters  $\mathbf{d}^0 = (\delta_{-1}^0, \delta_0^0, \dots, \delta_N^0, \delta_{N+1}^0)$ , we require  $U_N(x, 0)$  satisfying the following requirements

$$U_N(x, 0) = U(x_i, 0), \quad 0 \leq i \leq N, \quad (U_N)_x(a, 0) = 0, \quad (U_N)_x(b, 0) = 0.$$

The above conditions lead to  $A\mathbf{d}^0 = \mathbf{b}$  matrix equation, which is solved by using a variant of Thomas algorithm.

### 3. THE STABILITY ANALYSIS

We implement the Von Neumann stability analysis (Fourier mode method) in which the growth factor of a typical Fourier mode is defined as

$$\delta_j^n = \delta^{\wedge n} e^{ijkh}, \quad (10)$$

where  $k$  is the mode number and  $h$  is the element size. To apply Von Neumann stability analysis, The EW equation should be linearized by assuming that the quantity  $U$  in the nonlinear  $UU_x$  is locally constant. This is equivalent to having the corresponding values of the element parameters  $\delta_j$  in the equation (8) are also locally constant. Substituting equation (10) in the linearized recurrence relationship corresponding to equation (8) lead to

$\delta_j^{\wedge n+1} = \delta \delta_j^{\wedge n}$ , where the growth factor for mode  $k$  has the form

$$\delta = \frac{a - ib}{a + ib}, \quad \text{where } a = 4 + \frac{12k}{h^2} + \left(2 - \frac{12k}{h^2}\right) \cos(kh), \quad b = \frac{3\Delta t}{2h} U \sin(kh).$$

Since the magnitude of the growth factor is  $|\delta| = \sqrt{\delta \delta^{\wedge}} = 1$ , linearized system (8) is unconditionally stable.

### 4. NUMERICAL EXAMPLES AND RESULTS

In this section, studying the test problems concerned with migration validates the proposed method; undular bore development and generation of solitary waves by boundary forcing. Accuracy is measured using by the  $L_2$  and  $L_\infty$  error norms defined by  $\|U - U_N\|_2^2 = h \sum_{j=0}^N |(U_j - (U_N^n)_j)|^2$  and  $\|U - U_N\|_\infty = \max_j |U_j - (U_N^n)_j|$ .

In order to get reliable solitary solutions, discrete conservation laws are important features in computing smooth solutions of the EW equation. Since an efficient numerical scheme must keep the conservation properties of evolution equations constants, we will examine the three invariants of numerical solution, respectively, corresponding to the conservation of the mass, momentum and energy, which are given with following integrals [3]:

$$\begin{aligned} C_1 &= \int_a^b U dx \cong h \sum_{j=1}^N U_j^n, & C_3 &= \int_a^b U^3 dx \cong h \sum_{j=1}^N (U_j^n)^3, \\ C_2 &= \int_a^b (U^2 + \mu(U_x)^2) dx \cong h \sum_{j=1}^N (U_j^n)^2 + \mu((U')_j^n) \end{aligned} \quad (11)$$

The integrals are approximated by sums in (11) which correspond to an implementation of the trapezium rule for quadrature. The values  $U_j^n$ ,  $(U')_j^n$  and  $(U'')_j^n$  are computed from the eqs. (6) after finding parameters  $\delta_j^n$  from the system (8).

**(a)** The solitary wave solution of the eq. (1) is given by

$$U(x, t) = 3c \operatorname{sech}^2(k(x - x_0 - vt)), \quad \text{where } k = 1/2\sqrt{1/\mu}, \quad v = c.$$

This solution corresponds to a solitary wave of magnitude  $3c$  and  $k$  measures width of the wave, initially centered on the position  $x_0$  and propagate to the right

without change of shape at a steady velocity  $v$ . This equation takes name of the equal width equation due to all solitary waves of the same width. The initial condition is

$$U(x,0) = 3c \operatorname{sech}^2(k(x - x_0)). \tag{13}$$

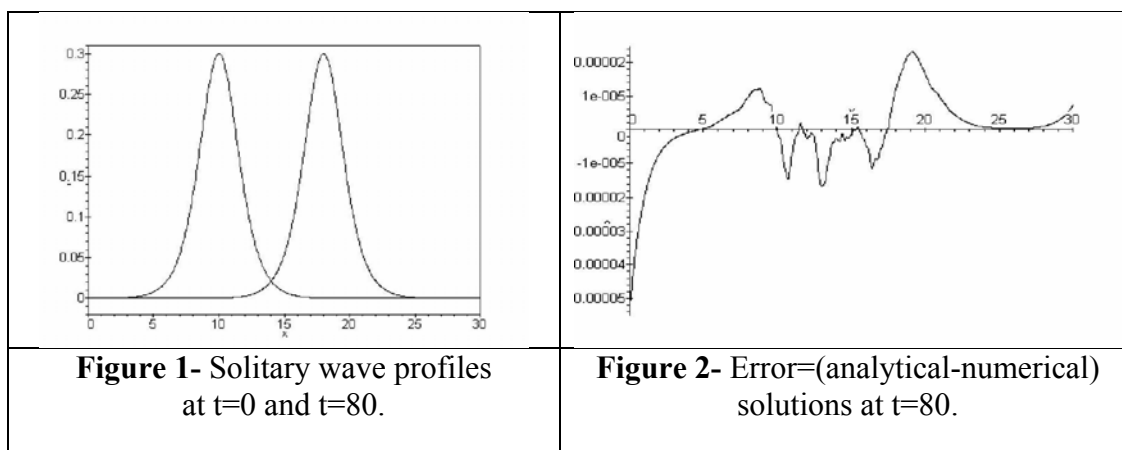
For the purpose of comparing with the earlier paper [9], parameters are chosen as  $c=0.1$ ,  $\mu = 1$ ,  $x_0 = 10$ ,  $\alpha_1 = 0$ ,  $\alpha_2 = 0$ . Range  $[0, 30]$  is divided into 400 elements of equal length  $h=0.03$  and time increment  $\Delta t = 0.05$  is used.  $L_2$  and  $L_\infty$  error norms and three invariants for the EW equation are recorded in Table 1 for times up to  $t=80$ . Initial condition and graphical solution of the single solitary wave is shown in Figure 1. From this graph, we say that a solitary wave moving to the right is simulated in its fairly original form as compared with the initial wave and the solution at the time  $t=80$ . The distribution of the errors at the mesh points at time  $t=80$  is shown graphically for a solitary wave of the amplitude 0.3 in Figure 2 from which largest error is concentrated near left boundary on the solution domain and oscillates between  $-4.8 \times 10^5$  and  $2.1 \times 10^5$ . Constants of the motion  $C_1, C_2, C_3$  may be evaluated analytically to give

$$C_1 = 6c/k = 1.2, \quad C_2 = 12c^2/k + 48kc^2\mu/5 = 0.288, \quad C_3 = 144c^3/5 = 0.0576.$$

Maximum change of invariants  $C_1, C_2, C_3$  varies from the analytical invariants by less than  $1.25 \times 10^{-5}$ ,  $2.5 \times 10^{-5}$ ,  $1.25 \times 10^{-5}$  percent for the presented scheme respectively whereas  $1.11 \times 10^{-2}$ ,  $3.13 \times 10^{-3}$ ,  $2.23 \times 10^{-3}$  percent at Gardner's scheme [9], during program running. In the same table, using the least-square method, the single solitary wave solution is presented when the time step is  $\Delta t = 0.03$ . Improvement is obtained for the  $L_2$  and  $L_\infty$  error norms when the cubic collocation method is used as compared with the results of the reference [9,10].

**Table 1-** Solitary wave amplitude 0.3,  $x_0 = 10$ ,  $h=0.03$ ,  $\Delta t = 0.05$ ,  $0 \leq x \leq 30$

Time	$C_1$	$C_2$	$C_3$	$L_2 \times 10^3$	$L_\infty \times 10^3$
0	1.19995	0.2880	0.05760	0.000	0.000
5	1.19999	0.2880	0.05760	0.021	0.033
10	1.20010	0.28804	0.05761	0.048	0.033
20	1.20015	0.28805	0.05761	0.064	0.046
40	1.20005	0.28800	0.05760	0.049	0.052
80	1.19998	0.28798	0.05759	0.056	0.053
80 ( $\Delta t = 0.03$ )	1.20010	0.28802	0.05761	0.132	0.078
80 (ref. [9])	1.1910	0.2855	0.05582	3.849	2.646
80 (ref. [10])	1.1964	0.2858	0.0569	7.444	4.373



To make the further comparison, the motion of the solitary wave with amplitude 3.0 is modelled and compare the results given in reference [6,9] at time  $t=40$  over the region  $0 \leq x \leq 80$ ; see Table 2 in which three conserved constants  $C_1, C_2, C_3$  and  $L_2, L_\infty$  error norms are recorded at various space-time step combinations. We find that more accurate results using proposed method are obtained than the Petrov-Galerkin scheme with the quadratic B-splines and least square finite element scheme but it has given a little bigger error than Galerkin scheme with the cubic B-splines in the  $L_2$  norm with choice of  $h=0.2$  and  $\Delta t=0.1$ . If we go for the smaller amplitude and make comparison in the table of the paper [6,9] with different time and space steps at time  $t=80$ , results are in Table 3 is documented and prosperity of the proposed scheme is verified for the various space-time combinations.

**Table 2-** Solitary wave amplitude 3.0,  $x_0 = 15$ ,  $0 \leq x \leq 80$ ; simulation results at  $t=40$ , various space - time combinations

h	$\Delta t$	$C_1$	$C_2$	$C_3$	$L_2 \times 10^3$	$L_\infty \times 10^3$
0.2	0.2	12.00060	28.80230	57.60610	252.869	138.0913
0.1	0.2	12.00050	28.80165	57.60463	222.500	119.8813
0.2	0.1	12.00010	28.80053	57.60130	95.670	53.9152
0.1	0.1	12.00023	28.80085	57.60250	63.380	34.6775
0.06667	0.05	12.00021	28.80143	57.60430	16.136	9.0130
0.05	0.05	11.99997	28.79944	57.59833	17.189	9.3597
0.04	0.04	12.00137	28.80644	57.61935	6.65184	3.9033
0.2 [6]	0.1	11.9999	28.7998	57.5995	54.2	
0.2 [9]	0.1	12.0001	28.7895	57.6018	123.8	

**Table 3-** Solitary wave amplitude 0.3,  $x_0 = 10$ ,  $0 \leq x \leq 30$ , simulation results at  $t=80$ , various space - time combinations

h	$\Delta t$	$C_1$	$C_2$	$C_3$	$L_2 \times 10^3$	$L_\infty \times 10^3$
0.025	0.015	1.19994	0.28796	0.05759	0.06699	0.05310
0.03	0.03	1.2001	0.28802	0.05761	0.13175	0.07749
0.04	0.02	1.19991	0.28794	0.05758	0.10591	0.06746
0.05	0.03	1.19997	0.28796	0.05759	0.17186	0.09125
0.06	0.04	1.20001	0.28799	0.05760	0.21388	0.13128
0.1	0.06	1.20003	0.28800	0.05760	0.44739	0.28253
0.03 [10]	0.03				7.44	4.37

(b) When a deeper stream of water flows into an area of the still water in a long horizontal channel, a bore is formed. To study development of an undular bore followed earlier author [1], the following initial condition is used:

$$U(x,0) = 0.5U_0(1 - \tanh((x - x_c)/d)) \tag{14}$$

where  $U(x,0)$  denotes the elevation of the water level above the equilibrium surface at time  $t=0.0$ ,  $d$  represent the slope between the still water and deeper water and magnitude  $U_0$  gives amount of the change in the water level and is centred on the  $x = x_c$ . In order to compute the numerical solution on the interval  $[a, b]$ , artificial boundary conditions  $U(a, t) = U_0, U(b, t) = 0$  are assumed to model the boundary conditions  $U \rightarrow 0$  as  $x \rightarrow \infty$  and  $U \rightarrow U_0$  as  $x \rightarrow -\infty$ .

First, algorithm is carried out up to time  $t=800$ . A range of  $a = -20 \leq x \leq b = 50$  with space step  $h=0.05$  and time step  $\Delta t = 0.05$  is taken with  $\mu = 0.1666667$ ,  $x_c = 0$  and  $d=5$  which are chosen to compare with results of the reference [9]. Table 4 contains the invariants  $C_1, C_2, C_3$  and position and amplitude of the leading undulation for the presented collocation method. Amplitude of the leading undulation measured as 0.184 at time  $t=800$ , which is in accord with the observation of the experiment of Gardner et al. [9]. Figure 3 shows both initial and undulation profiles at times  $t=0.0, 200, 400, 600, 800$ . The profile of the presented scheme at time  $t=400$  confirm the same profile of reference [9] of Figure 3. Variations of the invariants  $C_1, C_2, C_3$  can be worked out by the formulas [9];

$$\frac{dC_1}{dt} = \frac{d}{dt} \int_{-\infty}^{\infty} U dx = \frac{1}{2} U_0^2 = M_1, \quad \frac{dC_3}{dt} = \frac{d}{dt} \int_{-\infty}^{\infty} U^3 dx = \frac{3}{4} U_0^4 = M_3,$$

$$\frac{dC_2}{dt} = \frac{d}{dt} \int_{-\infty}^{\infty} (U^2 + \mu(U_x)^2) dx = \frac{2}{3} U_0^3 = M_2.$$

According to formulas, predicted theoretical values are calculated as  $M_1 = 5.03 \times 10^{-3}$ ,  $M_2 = 6.66667 \times 10^{-4}$ ,  $M_3 = 7.5 \times 10^{-5}$ . Numerical rates of change in invariants may be deduced from Table 4 that  $M_1 = 5.00065 \times 10^{-3}$ ,  $M_2 = 6.66639 \times 10^{-4}$ ,  $M_3 = 7.5005 \times 10^{-5}$ . These values are very close than the values quoted in the reference [9], which was calculated as  $M_1 = 5.03 \times 10^{-3}$ ,  $M_2 = 6.72 \times 10^{-4}$ ,  $M_3 = 7.59 \times 10^{-5}$ .

**Table 4-** Development of an undular bore  $d=5$ ,  $U_0 = 0.1$

Time	$C_1$	$C_2$	$C_3$	x	U
0	2.002579	0.175378	0.016277		
100	2.502395	0.242008	0.023772		
200	3.002354	0.308289	0.030866	8.80	0.16047
300	3.502342	0.375315	0.038440	14.50	0.17504
400	4.002584	0.442003	0.046274	20.40	0.17923
500	4.502592	0.508658	0.053774	26.05	0.18137
600	5.002832	0.575343	0.061277	32.50	0.18262
700	5.502838	0.641999	0.068777	38.60	0.18341
800	6.003096	0.708689	0.076281	44.75	0.18397
800 [9]	6.027221	0.713333	0.07700	44.7	0.18376

The algorithm with the above initial condition (14) by using a steeper initial wave parameters  $d=2$  is also rerun to get the three invariants and perspective views of undulation profiles; results are shown in Table 5.

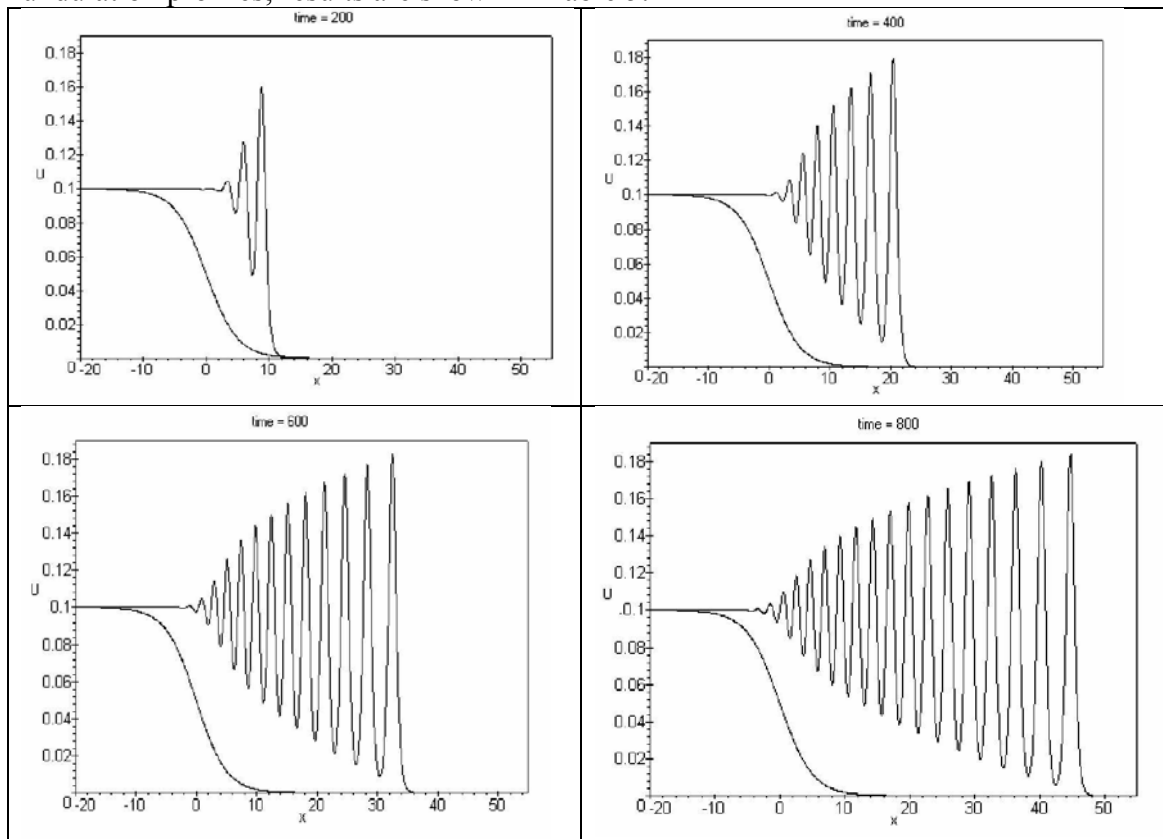


**Figure 3-** Initial profiles and undulation profiles with  $d=5$  at various times

Figure 4 shows the development of undular bores at times  $t=0.0, 200, 400, 600$  and  $800$  in that with a steeper initial wave, leading undulation becomes appeared earlier and the numbers of the undulation increased, at least more than two undulations when a steeper slope is chosen. The rates of increase in quantities  $C_1, C_2, C_3$  are calculated for choosing  $d=2$  as  $M_1 = 5.00087 \times 10^{-3}$ ,  $M_2 = 6.66674 \times 10^{-4}$ ,  $M_3 = 7.5011 \times 10^{-5}$ .

**Table 5-** Development of an undular bore  $d=2, U_0 = 0.1$

Time	$C_1$	$C_2$	$C_3$	x	U
0	2.002497	0.190528	0.018525		
100	2.502497	0.257189	0.026025	3.7	0.15724
200	3.002508	0.323846	0.033525	9.40	0.17597
300	3.502491	0.390499	0.041025	15.30	0.18007
400	4.002724	0.457183	0.048528	21.35	0.18201
500	4.502702	0.523833	0.056027	27.45	0.18314
600	5.002946	0.590522	0.063530	33.55	0.18367
700	5.502954	0.657177	0.071030	39.70	0.18428
800	6.003194	0.723867	0.078534	45.85	0.18460
800 [9]	5.944366	0.712677	0.076876	45.7	0.18392

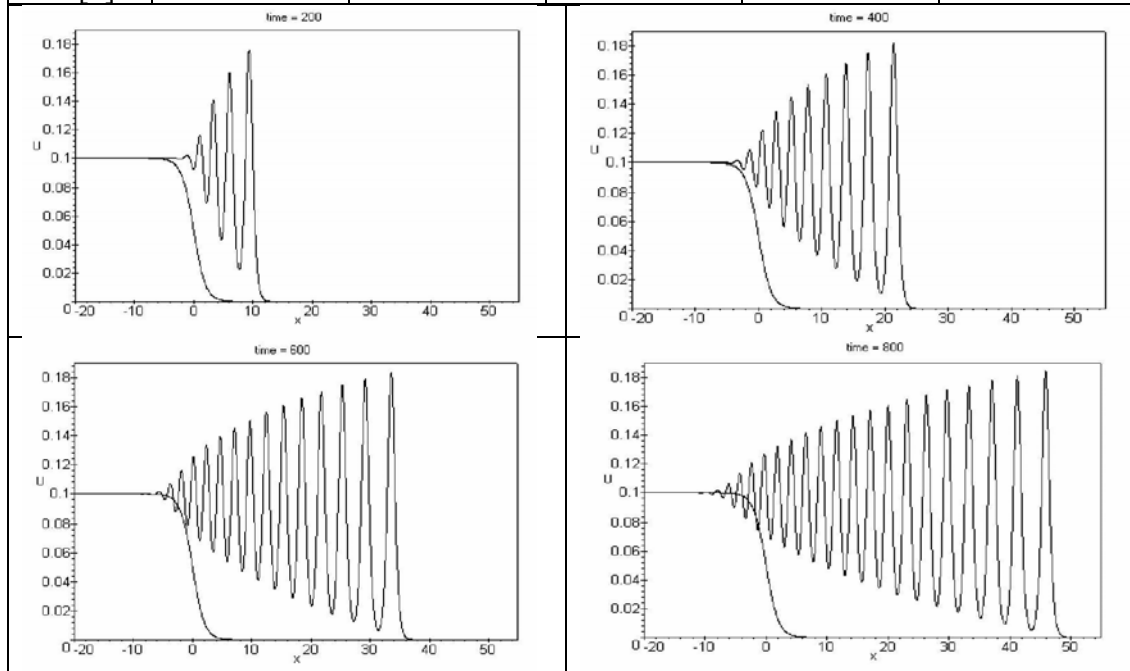


**Figure 4-** Initial profiles and undulation profiles with  $d=2$  at various times

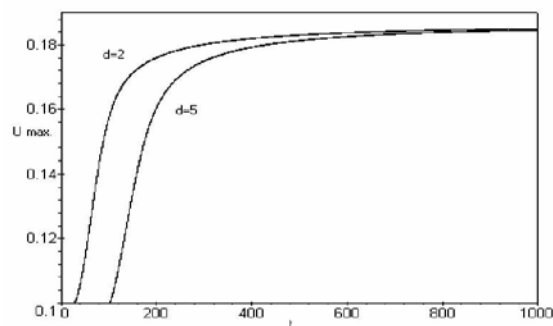


**Figure 5-** Growth in the amplitude of the leading undulations  $d=5$  and  $d=2$ .

Growth of the leading undulation for both gentle and steeper initial profiles is shown up to time  $t=1000$  over the region  $-20 \leq x \leq 1000$  in Figure 5, from which a limiting value has been observed. Limiting value of 0.184, which is the same with those obtained in the previous simulation [9] is recorded.

(c) Generation of the waves within a semi-infinite region is modelled by using the boundary condition at  $x=0$

$$U(x,0) = \begin{cases} U_0 \frac{t}{\tau} & , \quad 0 \leq t \leq \tau \\ U_0 & , \quad \text{otherwise} \end{cases}$$

where  $U(x, t)$  denotes the elevation of the surface above the equilibrium level and the steady forcing  $U_0 t/\tau$  is applied for short time period  $\tau$  to build up the constant impulse  $U_0$ . Boundary condition at far right end is required as  $U \rightarrow 0$  as  $x \rightarrow \infty$ . In the computation, the parameters  $\mu = 1$ ,  $h=0.2$ ,  $\Delta t = 0.05$ ,  $U_0 = 2$  are taken over the range  $0 \leq x \leq 120$ , which are selected to coincide with the paper [11]. The numerical experiment is run until time  $t=400$  and values of the amplitudes of the generated solitary waves are recorded at various times in the Table 6. In the same table, wave position and birth time of those waves are also given. Leading wave was started to appear at about time  $t=19$  whereas in the paper [11] the birth time of the leading wave was written to appear at time  $t=27$ . At early times of wave generation, we recorded higher amplitude of the generated waves than that of the reference [11]. For example at time  $t=30$ , maximum wave height of the leading waves is 1.384 whereas in Table 2 of the mentioned paper it is 1.11. Despite this, at time  $t=200$ , same numbers of solitary waves are produced and magnitudes of the solitary waves for the proposed method happened a little larger than that of reference [11] in the third digits mostly. The graphical solution at time  $t=400$  show that twenty-nine waves have been evolved as seen in Figure 7. In Figure 6 temporal development of the amplitudes of the generated waves at time  $t=200$  are graphed. From this figure we observed that waves amplitudes after the birth time increased sharply up to height =1.5 and than continued to grow steadily. New waves, after the first four waves birth times, are generated a time period of 13.25.

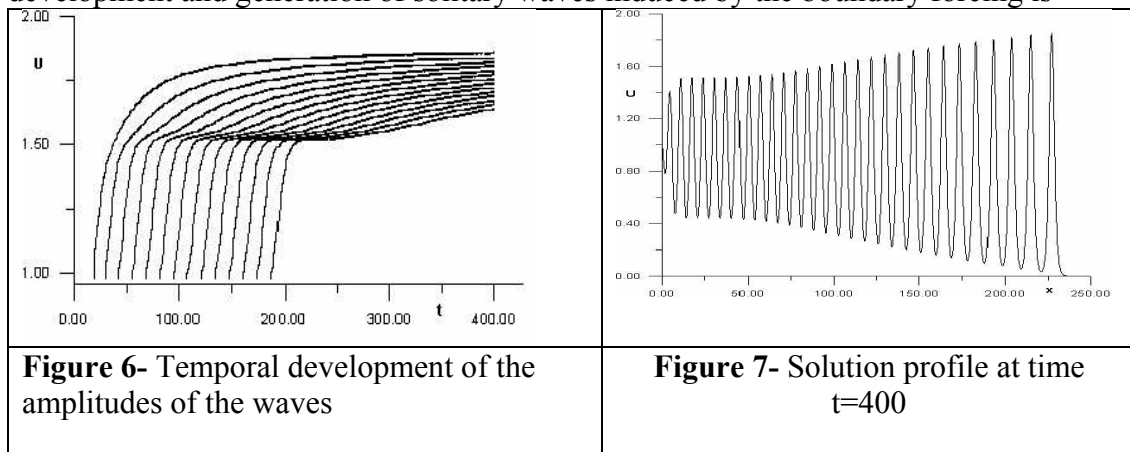
**Table 6-** Wave amplitudes  $U_0 = 1$ ,  $h=0.2$ ,  $\Delta t = 0.05$ ,  $0 \leq x \leq 120$

Time	1	2	3	4	5	6	7
30	1.384						
40	1.512	1.362					
50	1.593	1.500	1.265				
60	1.652	1.548	1.487	1.121			
70	1.695	1.592	1.525	1.452	1.011		
80	1.721	1.630	1.553	1.520	1.381		
100	1.764	1.691	1.616	1.552	1.529	1.489	1.122
120	1.790	1.726	1.663	1.603	1.550	1.531	1.514
140	1.806	1.751	1.698	1.646	1.593	1.551	1.531
200	1.832	1.793	1.765	1.724	1.687	1.652	1.617
200 [11]	1.81	1.77	1.74	1.70	1.67	1.63	1.59
400	1.852	1.838	1.821	1.803	1.787	1.770	1.754
Wave pos.	104.32	93.6	84.2	75.2	66.8	59.0	51.4

Birth time	19.25	30.8	43.25	56.049	69.2	82.45	95.70
Birth t. [11]	27.00	38.30	50.75	63.55	76.5	89.65	102.90
<b>Time</b>	<b>8</b>	<b>9</b>	<b>10</b>	<b>11</b>	<b>12</b>	<b>13</b>	<b>14</b>
120	1.375						
140	1.522	1.482	1.128				
200	1.581	1.553	1.536	1.52	1.517	1.506	1.381
200 [11]	1.54	1.51	1.51	1.51	1.51	1.48	1.12
400	1.736	1.721	1.703	1.684	1.669	1.653	1.637
Wave pos.	44.2	37.2	30.4	23.8	17.0	10.6	4.2
Birth time	108.952	122.253	135.504	148.754	162.005	175.256	188.507
Birth t. [11]	116.15	129.40	142.70	155.95	169.20	182.50	195.75

**5. CONCLUSIONS**

The cubic B-spline collocation method is set up to obtain numerical solution of the EW equation. The comparison of calculations shows that the proposed method is capable of producing better results than those schemes [10,11], but failed to emulate the results of the Galerkin finite element method. Simulation of the single solitary wave solution is faithfully represented in shape during running time. Undular bore development and generation of solitary waves induced by the boundary forcing is



modelled by using the EW equation. The results are illustrated to confirm existing work. The results suggest that proposed method, whose application is easier than many other numerical schemes such as finite element methods, Fourier spectral methods can be applied to this type of the nonlinear wave problems with success.

**REFERENCES**

1. D. H. Peregrine, Calculations of the development of an undular bore, *J. Fluid. Mech.* **25**, 321-330, 1966.
2. P. M. Prenter, *Splines and Variational methods*, Wiley, New York, 1975.
3. P. J. Olver, Euler operators and conservation laws of the BBM equations, *Math. Proc. Camb. Phil. Soc.* **85**, 143-159, 1979.
4. P. J. Morrison, J. D. Meiss and J. R. Carey, Scattering of RLW solitary waves, *Physica*, **11D**, 324-336, 1984.

5. L. R. T. Gardner and G. A. Gardner, Solitary waves of the regularized long wave equation, *J. Comput. Physics*. **91**, 441- 459, 1990.
6. L. R. T. Gardner and G. A. Gardner, Solitary waves of the equal width wave equation, *J. Comput. Physics*. **101**, 218-223, 1992.
7. L. R. T. Gardner, G. A. Gardner and İ. Dağ, A B-spline finite element method for the regularized long wave equation, *Commun. Numer. Methods Eng.*, **vol.11**, no 1, 59-68, 1995.
8. L. R. T. Gardner, G. A. Gardner and İ. Dağ, Boundary forced RLW equation, *Nuovo Cimento*, **10B**, 1487-1496, 1995.
9. L. R. T. Gardner, G. A. Gardner, F. A. Ayoub and N. K. Amein, Simulations of the EW undular bore, *Commun. Numer. Methods Eng.*, **13**, 583-592, 1997.
10. S. I. Zaki, A least-squares finite element scheme for the EW equation, *Comput. Met. Appl. Mech. Engrg.*, **189**, 587-594, 2000.
11. S. I. Zaki, Solitary waves induced by the boundary forced EW equation, *Comput. Met. Appl. Mech. Engrg.*, **190**, 4881-4887, 2001.